

Microstructure and pinning properties of hexagonal-disc shaped single crystalline MgB₂

C. U. Jung,* J. Y. Kim, P. Chowdhury, Kijoon H. P. Kim, and Sung-Ik Lee†
*National Creative Research Initiative Center for Superconductivity and Department of Physics,
 Pohang University of Science and Technology, Pohang 790-784, Republic of Korea*

D. S. Koh
Department of Physics, Pohang University of Science and Technology, Pohang 790-784, Republic of Korea

N. Tamura and W. A. Caldwell
*Lawrence Berkeley National Laboratory, Advanced Light Source,
 1 Cyclotron Road, MS-2-400 Berkeley, CA 94720, USA*

J. R. Patel
*Lawrence Berkeley National Laboratory, Advanced Light Source,
 1 Cyclotron Road, MS 7-222 Berkeley, CA 94720, USA,
 and SSRL/SLAC, Stanford University, CA 94309, USA*
 (Dated: November 8, 2018)

We synthesized hexagonal-disc-shaped MgB₂ single crystals under high-pressure conditions and analyzed the microstructure and pinning properties. The lattice constants and the Laue pattern of the crystals from X-ray micro-diffraction showed the crystal symmetry of MgB₂. A thorough crystallographic mapping within a single crystal showed that the edge and c-axis of hexagonal-disc shape exactly matched the (10-10) and the (0001) directions of the MgB₂ phase. Thus, these well-shaped single crystals may be the best candidates for studying the direction dependences of the physical properties. The magnetization curve and the magnetic hysteresis for these single crystals showed the existence of a wide reversible region and weak pinning properties, which supported our single crystals being very clean.

PACS numbers: 74.25.-q, 74.60.Ge, 74.72.-h

The recent discovery¹ of superconductivity in MgB₂ has attracted great scientific^{2,3} and industrial^{4,5} interest. Even though basic issues such as the carrier type² were addressed immediately, conflicting reports still exist, especially on the transport properties. For example, the residual resistivity ratio (RRR) of bulk MgB₂ ranges from 1.2 to 30.⁶

Higher quality bulk MgB₂ (called *highRRR-MgB₂*) has been claimed to have a higher values of RRR (20 ~ 25), a low residual resistivity ($\rho(40\text{ K}) < 1\ \mu\Omega\text{cm}$), a higher magneto-resistance (MR), and a resistivity upturn at low temperature under high magnetic field.³ Insulating impurities and/or local strains have been suggested as possible origins for these different observations.^{7,8,9,10,11} However, very recently, the existence of unreacted Mg successfully explained the unusual enhancement of the RRR and the MR in polycrystalline MgB₂.⁶

Compared to the wide distribution of the RRR for polycrystals, the RRR in the ab-plane resistivity for single crystals has a narrow distribution.^{12,13} The RRR of single crystals ranges from 5 to 6, which is much smaller than the values for *highRRR-MgB₂* bulk samples, but similar to the values for well-prepared polycrystals.^{6,14,15,16} The anisotropy factor ($\gamma \sim 3$) and the Debye temperature ($\Theta \sim 1160 \pm 60\text{ K}$) are also consistent among various reports.¹⁷

It is interesting to note that the magnetic properties

are somewhat different for different single crystals.^{12,13,18} The superconducting transition width in the zero-field-cooled magnetization for single crystals as large as a few hundred μm is a little bit broader than expected. The ratio of the low-field magnetization in the field-cooled (FC) state to that in the zero-field-cooled (ZFC) state gives a rough indication of the pinning strength, and this ratio is quite different for different single crystals. The magnetic hysteresis for single crystals having very weak pinning can be used to probe impurities. In one report, the magnetic hysteresis contained a significant amount of paramagnetic component. In another report, the magnetic hysteresis for an aggregation of single crystals showed a large ferromagnetic contribution and a significant irreversible magnetization.¹⁸

For the above reasons, it is necessary to confirm the quality of single crystals in more detail before performing the main measurements. The existence of impurities and structural imperfections on a microscopic scale can result in diverse physical properties. Here, we report the growth of, as well as X-ray micro-diffraction and magnetization measurements for, MgB₂ single crystals with hexagonal-disc shapes and shiny surfaces. Our single crystals are unique as far as the shape is concerned. The diagonal length and the thickness for the largest crystal was about 100 μm and 10 μm , respectively. The crystallinity was thoroughly identified by using the Laue pattern in the X-

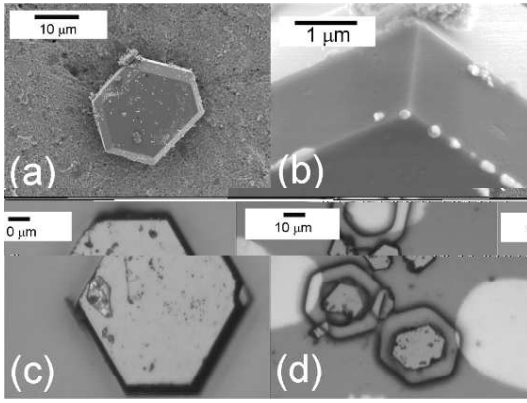


FIG. 1: SEM and polarizing optical microscope images of the MgB_2 single crystals with a hexagonal-disc shape. (a) MgB_2 made in a two-step process with a diagonal distance of about $25 \mu\text{m}$ and with a thickness of about $4 \mu\text{m}$. (b) High-resolution image at the corner of another crystal, and (c) polarizing optical microscope image of a single crystal grown in a one-step process. (d) Polarizing optical microscope images of MgB_2 single crystals. An epoxy was used to fix six single crystals at the center of $100\text{-}\mu\text{m}$ -wide Cu crosshairs.

ray micro-diffraction measurement. Both the edge and the c -axis of the hexagonally shape disc were found to match the crystal symmetry. The magnetization study showed that pinning was very weak for our hexagonal-disc-shaped single crystals.

Two different procedures were used to grow the single crystals, and in both cases, excess Mg was critical for the growth of single crystals. The first involved a two-step method in which already synthesized pieces of MgB_2 bulk¹⁹ were used as a seed material. They were heat treated in a Mg flux inside a Nb tube, which was sealed in an inert gas atmosphere. Then, the Nb tube was put inside a quartz tube, which was sealed in vacuum. The quartz tube was heated for one hour at 1050°C , cooled very slowly to 700°C for five to fifteen days, and then quenched to room temperature. The temperature dependences of the ab -plane resistivities for $H//ab$ and $H//c$ and high-resolution transmission electron microscope images have already been reported for the single crystals synthesized using this procedure.²⁰

In the one-step method, 1 : 1 mixtures of Mg and B powders were well ground and pressed into a pellet. Then, the pellet was placed in a Ta capsule. This capsule was put in a high-pressure cell equipped with a graphite heater. Heat treatment was done inside a 14-mm cubic multi-anvil-type press under 3 GPa.¹⁹ The heating temperature was around 1300°C . The temperature was maintained for about 30 minutes, and then was slowly lowered to $800 \sim 900^\circ\text{C}$. The final product was a pellet containing a mixture of single-crystalline MgB_2 and Mg flux.

It was found that the one-step method usually gave larger crystals, which was quite advantageous for the magnetization study in this research. The crystal images

were observed using a polarizing optical microscope and a field-emission scanning electron microscope (SEM). We successfully separated single-crystalline MgB_2 from the Mg flux by using a thermo-mechanical spinning method. This method is possible due to the fact that the melting (and/or decomposition) temperature of MgB_2 is higher than that of Mg.

Single crystals with sizes of tens of μm were selectively handled by using a homemade micro-tweezers and were fixed on Si substrates by using a photoresist as an epoxy. Since the volume of one crystal made in the one-step process was still rather small, we gathered about 200 single crystals on one substrate with their c -axes aligned perpendicular to the substrate surface.¹⁸ For the X-ray micro-diffraction measurements, several crystals were fixed at the center of Cu crosshairs on the substrate, as shown in Fig. 1(d).²⁰ The Cu crosshairs was used for the only purpose to facilitate the location of the sample by looking at the Cu fluorescence. The magnetic properties were measured with a SQUID magnetometer (Quantum Design, MPMS-XL).

The instrument used at the Advanced Light Source (ALS) for X-ray micro-diffraction is capable of producing a submicron-size X-ray microbeam and with submicron spatial resolution can probe the local texture in a single crystal.²¹ The sample was positioned using the Cu fluorescence signal detected from the Cu crosshairs on the Si substrate by using a high-purity Ge ORTEC solid-state detector connected to a multichannel analyzer. The crystal orientation with respect to the substrate can be determined with an accuracy of 0.01 degree.

Figure 1(a) shows a typical SEM image for a MgB_2 single crystal synthesized in a two-step process. The crystals observed by using a polarizing optical microscope had hexagonal-disc shapes with edge angles of 120 degrees and very flat and shiny surfaces. The sizes of the crystals were about $20 \sim 60 \mu\text{m}$ in diagonal length and $2 \sim 6 \mu\text{m}$ in thickness. Figure 1(b) shows a magnified view of the upper corner of another crystal. The smooth surfaces and the sharp edges confirm that our small crystals had a very low probability of having mosaic aggregates of nanocrystals either along the ab -plane or along the c -axis; thus, we had a better chance to study their intrinsic properties. The single crystals reported so far, except for those reported by us, have had irregular shapes.^{12,13,18}

Figure 1(c) shows a polarizing optical microscope image of a MgB_2 single crystal synthesized in a one-step process, which resulted in larger crystals. The sizes of these crystals were $30 \sim 100 \mu\text{m}$ in diagonal length, so they were picked for measurements of the magnetic properties and the X-ray micro-diffraction.

The crystal structure was identified by using white beam X-ray micro-diffraction measurements. After positioning these single crystals on the substrate in Fig. 1(d), a $100 \mu\text{m} \times 100 \mu\text{m}$ region between the Cu crosshairs was scanned with a step size of $2 \mu\text{m}$. At each step, the Laue pattern (together with the Cu K fluorescence signal) was collected with a BRUKER 6000 CCD camera which has

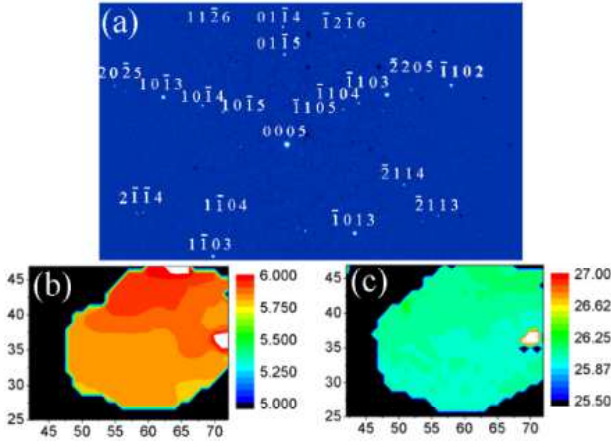


FIG. 2: (a) A representative image of an indexed Laue pattern from X-ray micro-diffraction. (b) and (c) are, respectively, for the out-of-plane and the in-plane orientations inside a single crystal. The out-of-plane orientation showed a variation of about 0.2 degrees between the bottom and the top parts, indicating a slight bending of the crystal. The in-plane orientation also showed slight inhomogeneities of up to about 0.2 degrees.

an active area of 9×9 cm and was placed about 4 cm above the sample. [2500 images, $1024 \text{ pixel} \times 1024 \text{ pixel}$ mode] The exposure time at each step, was 1 second. An example of a Laue pattern obtained from a MgB_2 single crystal is shown in Fig. 2. The Laue patterns are consistent with a hexagonal MgB_2 structure ($a = 3.086 \text{ \AA}$, $c = 3.524 \text{ \AA}$, Space Group number = 191, Ref. 1). The silicon reflections from the substrate were digitally removed. Typically, more than 20 reflections with energies ranging from 5 to 14 keV were indexed successfully. The (0005) reflection in the center of the pattern in Fig. 2 corresponds to the direction of the normal to the crystal surface. This confirms that the surface plane normal is along the c -axis. Moreover, the hexagonal edges of the crystals were found to match the $\langle 1,0,-1,0 \rangle$ directions within a fraction of a degree resolution. Thus, the shapes of the crystals in the microscope image followed the MgB_2 crystal symmetry, which will be quite useful for any research of the direction dependencies of the physical properties in MgB_2 .

Indexing the Laue patterns in Fig. 2(a) allowed us to calculate the complete orientation matrix of the X-ray illuminated volume. A finer step size of $1 \mu\text{m}$ was used for the white-beam scan. The orientation variations inside the single crystal shown in the right bottom corner of Fig 1(d) are shown in Figs. 2(b) and 2(c). Figure 2(b) is the out-of-plane orientation variation calculated as the angle between the c -axis and the normal to the surface of the silicon substrate. The out-of-plane variation was about 0.2 degrees between the light orange and the red regions. The out-of-plane orientation shows a variation of about 0.2 degrees between the bottom and the top parts, indicating a slight bending of the crystal (which might be due

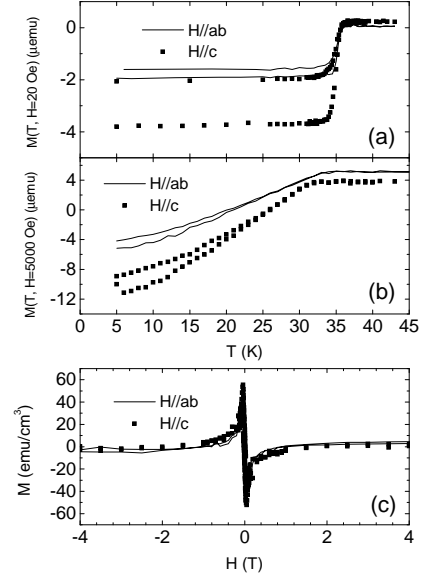


FIG. 3: (a) Low-field magnetization curve $M(T)$ measured at 20 Oe for $H//c$ and $H//ab$. (b) Magnetization curves measured at 5000 Oe showed a wide reversible region. $T_{\text{irr}}(H = 5000 \text{ Oe})$ was 26 and 24 K for $H//c$ and $H//ab$, respectively. (c) The magnetic hysteresis $M(H)$ at 5 K; the symbols and the line are for $H//c$ and $H//ab$, respectively.

to the photoresist used as an epoxy). Figure 2(c) shows the in-plane orientation variation calculated as the angle between the measured a -axis (or b -axis) and a reference directions. The variation was about 0.4 degrees between the light blue-green and the green regions. The in-plane orientation also showed some inhomogeneities of up to about 0.2 degrees.

These results demonstrate that the orientation of crystal axis of our hexagonal-disc-shaped single crystals was perfect, within 0.2 degrees. A recent study showed that (0001) twist grain-boundaries, formed by rotations along the c -axis (typically by about 4 degrees), were the major grain boundaries in polycrystalline MgB_2 .⁷ This kind of grain boundary was attributed to the weaker Mg-B bonding.⁷

To study the bulk nature of the superconductivity, we measured the magnetization curve $M(T)$ and the magnetic hysteresis $M(H)$. Figure 3(a) shows the magnetization curve $M(T)$ measured at 20 Oe in the ZFC and the FC states. The T_c onset was about 38 K. The FC signals for fields parallel and perpendicular to the c -axis were larger than 60% of the ZFC signals, which suggested that the pinning was very weak. The overall shape was not much different for these two orientations. The different values of the magnetic moment for the different field directions were due to a demagnetization effect caused by the planar-disc shapes of the crystals.²⁰ The transition width in the $M(T)$ curve was much narrower than that for single crystals made in the two-step method.²⁰ The volumes of the crystals made in the one-step process were about one order of magnitude larger than the

volumes of the crystals made in the two-step process.

The weak pinning was demonstrated by the magnetization at 5000 Oe and the magnetic hysteresis $M(H)$ at 5 K, as shown in Fig. 3(b) and (c), respectively. With $(M(H^-) - M(H^+)) = 0.1 \text{ emu/cm}^3$ as the criterion for the reversible point, the values of $T_{\text{irr}}(H = 5000 \text{ Oe})$ were 26 and 24 K for $H//c$ and $H//ab$, respectively. At each temperature, the upper critical fields obtained from the resistivity measurements were about 1.7 and 6 Tesla for our well-shaped single crystals.²⁰ Thus, a very wide reversible region existed in our single crystals, especially for $H//ab$. [H_{irr} for bulk MgB_2 at $T = 25 \text{ K}$ was about 3 T^{16} , which is about 6 times higher than that of single crystalline MgB_2 .]

The weak pinning shown by the wide reversible region was also consistent with the results of the $M(H)$ measurement. The $M(H)$ at 5 K in Fig. 3(c) showed negligible paramagnetic or ferromagnetic background up to 5 Tesla. Reversible magnetization was dominant for the $M(H)$ of our single crystals, which was quite consistent with fact that the pinning in our single crystals was weak and with the existence of wide reversible region demonstrated by the lower H_{irr} value in Fig 3(b). The different slopes of the $M(H)$ curves at the starting low fields ($H < 300 \text{ Oe}$) for the different field directions were due to different demagnetization factors.

Previously, the $M(H)$ for irregular shaped single crystals was shown to have a non-negligible irreversible contribution¹⁸ and a quite large paramagnetic and/or ferromagnetic background signal, which might have been due to the existence of impurities.^{13,18} The results in Fig. 3 indicate that the strong bulk pinning previously reported for polycrystalline²² and thin films⁴ might be due

to entirely extrinsic pinning sites, such as grain boundaries and crystallographic defects.²³ This is consistent with the absence of core pinning, even at $T \sim 0.5 \times T_c$, for bulk sample.⁵

In summary, we report the structural and magnetic properties of MgB_2 single crystals with hexagonal-disc shapes. The X-ray micro-diffraction showed that the hexagonal-disc shape of the single crystal followed the crystallographic symmetry, which will be very useful for studying orientation-dependent physical properties. The magnetization curve and the magnetic hysteresis provided consistent evidence that our single crystals were very clean and had very weak pinning: the large FC magnetization and the sharp transition of the ZFC magnetization at low field $M(T)$, the wide reversible region, and the $M(H, T = 5 \text{ K})$ dominated by the reversible magnetization without any significant paramagnetic and/or ferromagnetic contribution.

Acknowledgments

We appreciate M. H. Kim and S. R. Jung for their help in handling of tiny crystals. This work is supported by the Ministry of Science and Technology of Korea through the Creative Research Initiative Program. The Advanced Light Source is supported by the Director, Office of Science, Office of Basic Energy Sciences, Materials Sciences Division, of the U.S. Department of Energy under Contract No. DE-AC03-76SF00098 at Lawrence Berkeley National Laboratory.

* New address: Tokura Spin Superstructure Project, ER-ATO, JST, AIST, Tsukuba Central 4 Tsukuba, Ibaraki 305-8562, Japan; E-mail: cu-jung@aist.go.jp; Url: <http://unit.aist.go.jp/cerc/>

† E-mail: silee@postech.ac.kr; Url: <http://www-psc.postech.ac.kr>

¹ J. Nagamatsu, N. Nakagawa, T. Muranaka, Y. Zenitani, and J. Akimitsu, *Nature* **410**, 63 (2001).

² W. N. Kang, C. U. Jung, Kijoon H. P. Kim, Min-Seok Park, S. Y. Lee, Hyeong-Jin Kim, Eun-Mi Choi, Kyung Hee Kim, Mun-Seog Kim, and Sung-Ik Lee, *Appl. Phys. Lett.* **79**, 982 (2001).

³ S. L. Bud'ko, C. Petrovic, G. Lapertot, C. E. Cunningham, P. C. Canfield, M-H. Jung, and A. H. Lacerda, *Phys. Rev. B* **63**, 220503 (2001); D. K. Finnemore, J. E. Ostenson, S. L. Bud'ko, G. Lapertot, and P. C. Canfield, *Phys. Rev. Lett.* **86**, 2420 (2001).

⁴ W. N. Kang, Hyeong-Jin Kim, Eun-Mi Choi, C. U. Jung, and Sung-Ik Lee, *Science* **292**, 1521 (2001).

⁵ D. C. Larbalestier, L. D. Cooley, M. O. Rikel, A. A. Polyan-skii, J. Jiang, S. Patnaik, X. Y. Cai, D. M. Feldmann, A. Gurevich, A. A. Squitieri, M. T. Naus, C. B. Eom, E. E. Hellstrom, R. J. Cava, K. A. Regan, N. Rogado, M. A.

Hayward, T. He, J. S. Slusky, P. Khalifah, K. Inumaru, and M. Haas, *Nature* **410**, 186 (2001).

⁶ C. U. Jung, Heon-Jung Kim, Min-Seok Park, Mun-Seog Kim, J. Y. Kim, Zhonglian Du, Sung-Ik Lee, K. H. Kim, J. B. Betts, M. Jaime, A. H. Lacerda, and G. S. Boebinger, submitted to *Physica C*; K. H. Kim *et al.* (unpublished).

⁷ Y. Zhu, L. Wu, V. Volkov, Q. Li, G. Gu, A. R. Moodenbaugh, M. Malac, M. Suenaga, and J. Tranquada, *Physica C* **356**, 239 (2001).

⁸ X. H. Chen, Y. S. Wang, Y. Y. Xue, R. L. Meng, Y. Q. Wang, and C. W. Chu, *Phys. Rev. B* **65**, 024502 (2002).

⁹ Y. Y. Xue, R. L. Meng, B. Lorenz, J. K. Meen, Y. Y. Sun, and C. W. Chu, *cond-mat/0105478* (2001).

¹⁰ B. Lorenz, Y. Y. Xue, R. L. Meng, and C. W. Chu, *cond-mat/0110125* (2001).

¹¹ A. Serquis, Y. T. Zhu, E. J. Peterson, J. Y. Coulter, D. E. Peterson, and F. M. Mueller, *Appl. Phys. Lett.* **79**, 4399 (2001).

¹² S. Lee, H. Mori, T. Masui, Yu. Eltsev, A. Yamamoto, and S. Tajima, *J. Phys. Soc. Jpn.* **70**, 2255 (2001).

¹³ M. Xu, H. Kitazawa, Y. Takano, J. Ye, K. Nishida, H. Abe, A. Matsushita, N. Tsujii, and G. Kido, *Appl. Phys. Lett.* **79**, 2779 (2001); A. K. Pradhan, Z. X. Shi, M. Tokunaga,

- T. Tamegai, Y. Takano, K. Togano, H. Kito, and H. Ihara, Phys. Rev. B **64**, 212509 (2001).
- ¹⁴ N. A. Frederick, S. Li, M. B. Maple, V. F. Nesterenko, and S. S. Indrakanti, Physica C **363**, 1 (2001).
- ¹⁵ S. S. Indrakanti, V. F. Nesterenko, M. B. Maple, N. A. Frederick, W. M. Yuhasz, and Shi Li, Phil. Mag. Lett. **81**, 849 (2001).
- ¹⁶ G. Fuchs, K. -H. Müller, A. Handstein, K. Nenkov, V. N. Narozhnyi, D. Eckert, M. Wolf, and L. Schultz, Solid State Commun. **118**, 497 (2001).
- ¹⁷ However, even in single crystals, some spectra for the transport properties still exist. MR values at 5 T ranged from about 2% to 20% and the MR ratio for the two magnetic field directions shows a wide variation among reports.
- ¹⁸ O. F. de Lima, R. A. Ribeiro, M. A. Avila, C. A. Cardoso, and A. A. Coelho, Phys. Rev. Lett. **86**, 5974 (2001).
- ¹⁹ C. U. Jung, Min-Seok Park, W. N. Kang, Mun-Seog Kim, Kijoon H. P. Kim, S. Y. Lee, and Sung-Ik Lee, Appl. Phys. Lett. **78**, 4157 (2001); C. U. Jung, J. Y. Kim, Min-Seok Park, Heon-Jung Kim, Mun-Seog Kim, and Sung-Ik Lee, cond-mat/0106441 (2001).
- ²⁰ Kijoon H. P. Kim, Jae-Hyuk Choi, C. U. Jung, P. Chowdhury, Min-Seok Park, Heon-Jung Kim, J. Y. Kim, Zhonglian Du, Eun-Mi Choi, Mun-Seog Kim, W. N. Kang, Sung-Ik Lee, Gun Yong Sung, and Jeong Yong Lee, Phys. Rev. B **65**, 100510 (2002).
- ²¹ A. A. MacDowell, R. S. Celestre, N. Tamura, R. Spolenak, B. C. Valek, W. L. Brown, J. C. Bravman, H. A. Padmore, B. W. Batterman, and J. R. Patel, Nucl. Instrum. Meth. A **467-468**, 936 (2001).
- ²² Mun-Seog Kim, C. U. Jung, Min-Seok Park, S. Y. Lee, Kijoon H. P. Kim, W. N. Kang, and Sung-Ik Lee, Phys. Rev. B **64**, 12511 (2001).
- ²³ M. Pissas, E. Moraitakis, D. Stamopoulos, G. Papavassiliou, V. Psycharis, and S. Koutandos, cond-mat/0108153 (2001).